Enhanced Recognition of Single-Base Mismatch Using Locked Nucleic Acid-Integrated Hairpin DNA Probes Revealed by Atomic Force Microscopy Nanolithography

ARTICLE *in* ANALYTICAL CHEMISTRY · FEBRUARY 2010

Impact Factor: 5.64 · DOI: 10.1021/ac902665c · Source: PubMed

8 AUTHORS, INCLUDING:

Shin-Mou Wu
National Sun Yat-sen University
6 PUBLICATIONS **38** CITATIONS
SEE PROFILE

Cheng-Lung Chen
National Sun Yat-sen University
35 PUBLICATIONS **318** CITATIONS
SEE PROFILE

Anal. Chem. **2010,** *82,* 2395–2400

Enhanced Recognition of Single-Base Mismatch Using Locked Nucleic Acid-Integrated Hairpin DNA Probes Revealed by Atomic Force Microscopy Nanolithography

Wen-Hsin Han, Jun-Min Liao, Kuan-Liang Chen, Shin-Mou Wu, Yi-Wen Chiang, Shu-Ting Lo, Cheng-Lung Chen, and Chao-Ming Chiang*

Department of Chemistry, Center for Nanoscience and Nanotechnology, National Sun Yat-Sen University, Kaohsiung, Taiwan 80424

Probe design is a critical parameter in successful DNA and RNA target detection. In this proof-of-concept study, we evaluated the single-base mismatch recognition power of surface immobilized and self-assembled stem-loop hairpin DNA oligonucleotide probes modified to contain locked nucleic acid residues (LNA-HP). The stiffness change in conjunction with the stem opening of the interfacial molecules before and after hybridization led to clear variations of the overall film thickness or miniaturized nanospot height, which could be directly measured using an atomic force microscopy (AFM) nanolithography technique. Particularly, LNA-HP achieved highly differentiable readouts between perfectly complementary and singly mismatched targets (discrimination ratio as high as 2 to 3), outperforming the selectivity of its linear and hairpin counterparts with no LNA modification.

Sequence-specific interactions between target DNA or RNA in solution and nucleic acid probes immobilized on a surface form the fundamental basis for microarray biosensor technologies. Besides high affinity, high selectivity of probe−target hybridization, namely discrimination between very similar homologous sequences, becomes increasingly demanded due to the surge of interest in single nucleotide polymorphisms (SNPs)[1] as well as microRNA (miRNA)[2] detections. For example, the small size of miRNAs (18 to 24 mers) often makes selective base pairing difficult because the annealing temperature is low, thereby weakening the stringency of hybridization and greatly escalating the risk of cross hybridization. The major challenge is, thus, to design a recognition component which is "smart" enough to distinguish targets with a mismatch of as little as a single base and to simultaneously provide a sensitive signaling mechanism to translate the different hybridization events (perfect match vs mismatch) into differentiable readout. One approach is to design the oligonucleotide probe to fold onto itself, forming a hairpin (HP). This unique architecture provides a long loop portion to function as the recognizing element and a short stem hybrid to maintain the closed configuration. Upon hybridization, the target nucleotides find their favorable binding sequence in the loop, resulting in the formation of a rigid rodlike double helix and stem opening. As opposed to the conventional linear (LN) probe, such a deliberate secondary structure enhances sequence selectivity since the intermolecular probe−target hybridization needs to overcome the intramolecular unzipping of the stem base pairs.[3] This added competing factor renders more discernible rates and equilibrium amounts of captured targets between perfectly matched and singly mismatched cases.[4] Another strategy involves locked nucleic acid (LNA), a conformationally restricted nucleic acid analogue in which the ribose ring is "locked" with a methylene bridge connecting the 2′-O atom with the 4′-C atom, thus increasing the melting temperature (T_m) of the nucleic acid duplex by 4−8 °C per LNA monomer when integrated into one strand.[5,6] Noteworthy is that LNA/DNA hybrids possess very thin tolerance to the introduction of a single mismatch, causing T_m to plunge. Kurita et. al in their theoretical calculations showed that the T_m reduction for the mismatch-bearing LNA/DNA is much greater than that for the DNA/DNA (ΔT_m = 26 °C vs 10 °C for a single T-G mismatch within octameric double strands).[7]

To benefit from the biophysical properties offered by the stem-and-loop structure as well as LNA modification, Tan and coworkers pioneered the combined approach in the context of locked nucleic acid molecular beacon (LNA-MB) in solution-phase hybridization.[8] Aiming for the synergistic effect on the mismatch discrimination, here we investigate surface-bound capture probes with LNA coupled into HP oligonucleotide (LNA-HP). Similar to Tan's design, the hairpin consists of a 19-mer loop (fit the size of miRNAs) and a 6-mer stem. However, instead of a full modifica-

* Corresponding author. Phone: 886-7-5253939. Fax: 886-7-5253908. E-mail: cmc@mail.nsysu.edu.tw.

(1) Schafer, A. J.; Hawkins, J. R. *Nat. Biotechnol.* **1998**, *16*, 33–39.
(2) Nelson, P. T.; Baldwin, D. A.; Scearce, L. M.; Oberholtzer, J. C.; Tobias, J. W.; Mourelatos, Z. *Nat. Methods* **2004**, *1*, 155–161.
(3) Gao, Y.; Wolf, L. K.; Georgiadis, R. M. *Nucleic Acids Res.* **2006**, *34*, 3370–3377.
(4) Riccelli, P. V.; Merante, F.; Leung, K. T.; Bortolin, S.; Zastawny, R. L.; Janeczko, R.; Benight, A. S. *Nucleic Acids Res.* **2001**, *29*, 996–1004.
(5) Kaur, H.; Arora, A.; Wengel, J.; Maiti, S. *Biochemistry* **2006**, *45*, 7347–7355.
(6) McTigue, P. M.; Peterson, R. J.; Kahn, J. D. *Biochemistry* **2004**, *43*, 5388–5405.
(7) Natsume, T.; Ishikawa, Y.; Dedachi, K.; Tsukamoto, T.; Kurita, N. *Chem. Phys. Lett.* **2007**, *446*, 151–158.
(8) (a) Wang, L.; Yang, C. J.; Medley, C. D.; Benner, S. A.; Tan, W. *J. Am. Chem. Soc.* **2005**, *127*, 15664–15665. (b) Yang, C. J.; Wang, L.; Wu, Y.; Kim, Y.; Medley, C. D.; Lin, H.; Tan, W. *Nucleic Acids Res.* **2007**, *35*, 4030–4041.

10.1021/ac902665c
Published on Web 02/22/2010

Scheme 1. Design of Probe and Target Oligonucleotides

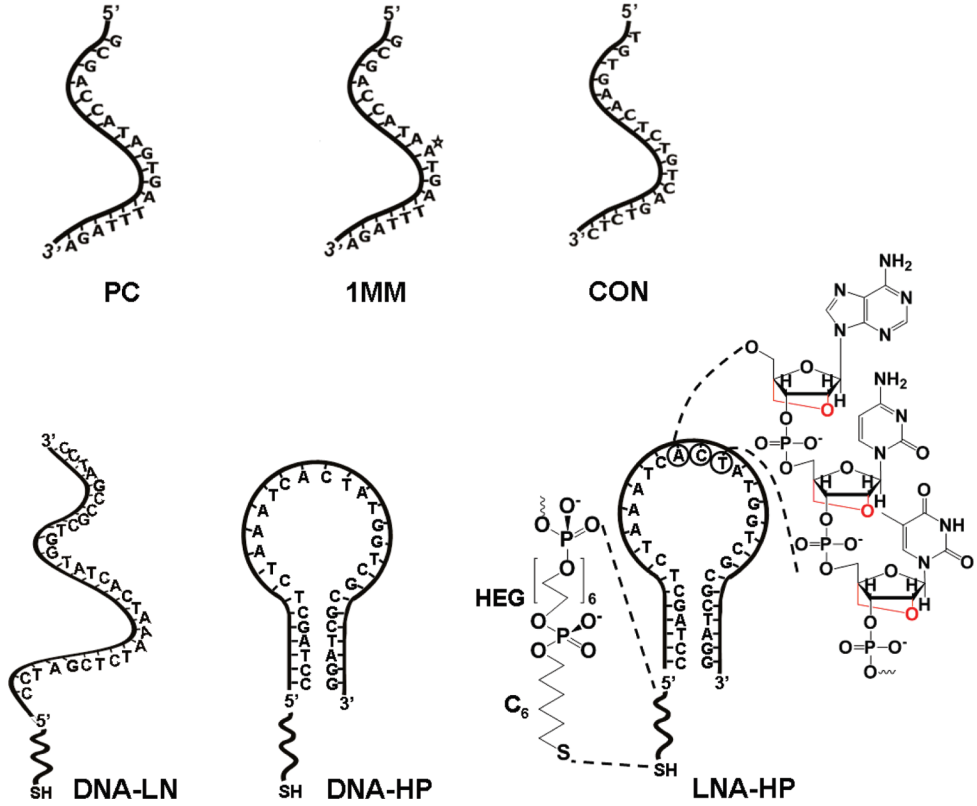

tion, we strategically place a triplet of LNA substitution surrounding the potential single-base mismatch site close to the center of the loop. This moderate LNA-modification is to keep the T_m not too high (T_m = 61.8 °C) such that room temperature target-loop annealing can still occur at reasonable rates.[9] Also such a triplet LNA design has been claimed by Owczarzy et al.[10] to exhibit the highest discriminatory power when the mismatch position and its two nearest-neighbor nucleotides are together LNA modified. The internal mismatch site is so chosen because the impact of single point mutation on the duplex binding affinity depends predominantly on position, largest in the middle of the sequence motif.[11,12] To evaluate the performance of LNA-HP, the corresponding hairpin oligonucletide without LNA alteration (DNA-HP) and a 31-mer single-stranded linear (random coil) DNA probe (DNA-LN) (the inner 19 bases are identical but the 6 bases at each opposing end are not self-complementary) serve as the contrasts. All three probe oligonucleotides are modified with thiol at their 5′ end in order to self-assemble onto a gold substrate. It is known that the further a confined biorecognizing functionality is away from the surface the more likely it is to interact freely with dissolved target molecules. We have the thiol group linked to oligo via not only the commonly used hexamethylene (C_6) moiety but also a supplementary hexaethylene glycol (HEG) spacer which is highly hydrophilic, so additional chain flexibility is endowed.[13] Target molecules include 19-mer single-stranded DNA oligonucleotides, (1) perfectly complementary (PC), (2) noncomplementary (CON as the control) to the interior region of the probes, and (3) oligomer bearing one mismatched base (substituting A* for G near the center (1MM)). Scheme 1 identifies the sequences of these probes and targets.

EXPERIMENTAL SECTION

Probe and Target Oligonucleotides. Oligonucleotides used in this work were custom-made by Integrated DNA Technologies (IDT). The thiol-derivatized oligonulceotides were received as disulfides, treated with solid-phase dithiothreitol (DTT, Merck) immediately prior to use, and purified with NAP-10 columns. The buffer used for the solution assembly of the probe layers was pH 7.5 and contained 1.0 M NaCl (MP Biochemical), 10 mM Tris-HCl, and 0.1 mM EDTA (IDT). Nuclease-free distilled water (Invitrogen) was used for all aqueous solutions and rinsing.

Surface. The gold-coated arrandee substrate is made of 250 nm final Au layer and 2.5 nm Cr adhesive layer on 0.7 mm thick 11 × 11 mm size borosilicate glass. By butane flame annealing, Au(111) terraces can be repeatedly obtained. Contact mode atomic force microscopy (AFM) characterization of the freshly prepared surface was then carried out, and only the surfaces having a peak-to-valley roughness of less than 1 nm were considered for assembly of the oligonucleotide probe or matrix layers.

Self-Assembly Process. Gold-coated substrate were immersed in 1 μM probe oligonucleotide solutions in 1 M NaCl-TE at room temperature for 2 h to allow for the adsorption and assembly of the recognition monolayer. In the case of making

(9) The optimal annealing was found to occur about 25 °C below T_m; see: Marmur, J.; Doty, P. *J. Mol. Biol.* **1961**, *3*, 585–594.
(10) You, Y.; Moreira, B. G.; Behlke, M. A.; Owczarzy, R. *Nucleic Acids Res.* **2006**, *34*, e60.
(11) Naiser, T.; Ehler, O.; Kayser, J.; Mai, T.; Michel, W.; Ott, A. *BMC Biotech.* **2008**, *8:48*.
(12) Hansen, K. M.; Ji, H.-F.; Wu, G.; Datar, R.; Cote, R.; Majumdar, A.; Thundat, T. *Anal. Chem.* **2001**, *72*, 1567–1571.
(13) Peeters, S.; Stakenborg, T.; Reekmans, G.; Laureyn, W.; Lagae, L; Aerschot, A. V.; Ranst, M. V. *Biosens. Bioelectron.* **2008**, *24*, 72–77.

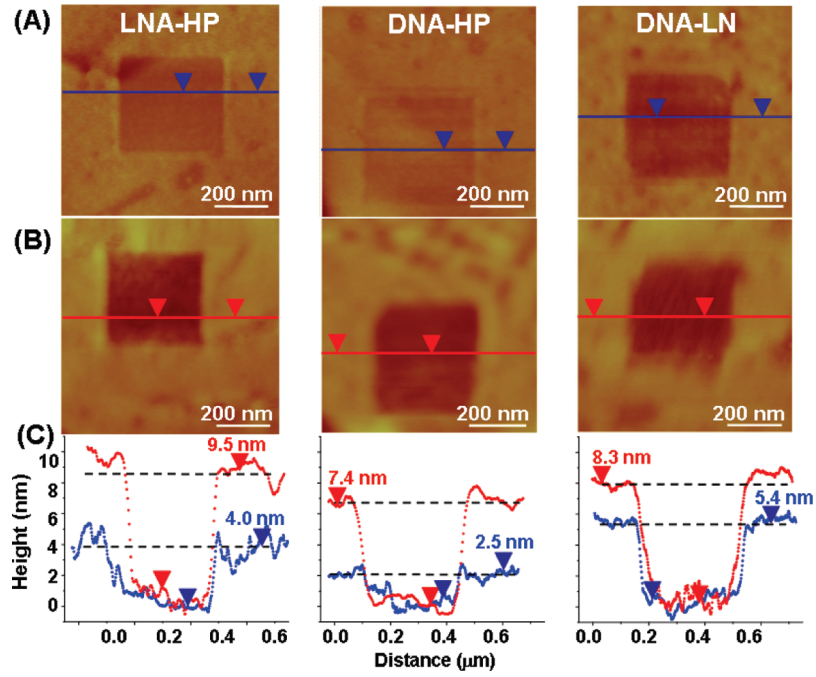

Figure 1. Representative AFM topographic images of various surface probe molecules (A) before and (B) after incubation with PC targets for 40 h. Nanoholes were made by AFM tip shaving within the films to reveal the thickness of each self-assembled monolayer (SAM). (C) Line profiles show changes in the depth of the holes due to base-pair recognition. Δh's are 5.5 ± 0.3, 4.9 ± 0.4, and 2.9 ± 0.6 nm, respectively. (Detailed AFM image sequence in the course of hybridization can be found in Figure S2 in the Supporting Information.)

the dense 12-mer double-stranded DNA matrix, the immersion time was increased to 40 h. After the specified time, samples were removed from the solution and rinsed thoroughly in nuclease-free water to remove loosely bound molecules and buffer salts.

Atomic Force Microscope. All AFM experiments were carried out on a MultiMode atomic force microscope with the NanoScope IIIa controller (Veeco) and a glass liquid cell of a fluid volume approximately 250 μL under TE buffer at 25 °C in contact mode. Si_3N_4 cantilevers (spring constant: 0.08 N/m, PNP-TR Nanoworld) were used in all image collection and nanolithography. Topographic images were recorded at minimum vertical tip forces by decreasing the set point until the tip disengaged from the surface and then reintroducing it with the minimum force required to achieve a stable image. Continual adjusting of the cantilever deflection feedback set point was often needed to compensate for thermal drifting. Height images were collected at 2 Hz and analyzed using the NanoScope analyzing software with first order flattening. Nanoshaved holes within the recognition or matrix layers were prepared by scanning the tip at a preselected small flat area. The chosen area was repeatedly scanned at 9 to 10 Hz under high loading force by advancing the set point several units to scratch away the tethered interfacial oligonucleotide molecules.

RESULTS AND DISCUSSION

Hybridization of Self-Assembled Monolayers. Immobilization of probes was achieved by incubation of each gold substrate (arrandee) for 2 h with a 1.0 μM buffered solution (1.0 M NaCl-TE) containing the thiol-derivatized oligonulceotides. The classic technique of adding short-chain hydroxyl-terminated alkanethiols, passivating the gold surface from nonspecifically binding with the amine groups in the bases of the oligos,[14] was not practiced in this work because the study by Keating et. al found that the benefit of improving the hybridization efficiency via surface dilution is less imperative for hairpin-type probes.[15] Despite the existing transduction mechanisms for DNA hybridization (optical, electrochemical, and mass-sensitive),[16] AFM-based methods emerge as a powerful alternative[12,17,18] and may be best suited for miniaturization. Work on sensitive detection of DNA hybridization at the nanoscale, combining AFM lithography (nanoshaving and nanografting)[19] and imaging, was elegantly demonstrated by research groups led by Holmberg,[20] Liu,[21] Abell,[22] Stambouli,[23] Casari,[24] and Scoles.[25] The common concept behind their work resides in the change of persistence length or stiffness of the interfacial molecules due to the switch of oligonucleotides from flexible single strands to rigid double strands before and after hybridization. As a result, the overall film thickness varies, that is measurable by AFM and proven to correlate with the extent of

(14) Herne, T. M; Tarlov, M. J. *J. Am. Chem. Soc.* **1997**, *119*, 8916.

(15) Cederquist, K. B.; Golightly, R. S.; Keating, C. D. *Langmuir* **2008**, *24*, 9162–9171.
(16) Teles, F. R. R.; Fonseca, L. P. *Talanta* **2008**, *77*, 606–623.
(17) Wang, J.; Bard, A. J. *Anal. Chem.* **2001**, *73*, 2207–2212.
(18) Jin., Y.; Wang, K.; Tan, W.; Wu, P.; Wang, Q.; Huang, H.; Huang, S.; Tang, Z.; Guo, Q. *Anal. Chem.* **2004**, *76*, 5721–5725.
(19) Liu, G.-Y.; Xu, S.; Qian, Y. *Acc. Chem. Res.* **2000**, *33*, 457–466.
(20) Holmberg, M.; Kühle, A.; Garnæs, J.; Boisen, A. *Ultramicroscopy* **2003**, *97*, 257–261.
(21) Liu, M.; Liu, G.-Y. *Langmuir* **2005**, *21*, 1972–1978.
(22) (a) Zhou, D.; Sinniah, K.; Abell, C.; Rayment, T. *Langmuir* **2002**, *18*, 8278–8281. (b) Zhou, D.; Sinniah, K.; Abell, C.; Rayment, T. *Angew. Chem., Int. Ed.* **2003**, *42*, 4934.
(23) Lavalley, V.; Chaudouët, P.; Stambouli, V. *Surf. Sci.* **2007**, *601*, 5424–5432.
(24) Baserga, A.; Viganò, M.; Casari, C. S.; Turri, S.; Bassi, A. L.; Levi, M.; Bottani, C. E. *Langmuir* **2008**, *24*, 13212–13217.
(25) Mirmomtaz, E.; Castronovo, M.; Grunwald, C.; Bano, F.; Scaini, D.; Ensafi, A. A.; Scoles, G.; Casalis, L. *Nano Lett.* **2008**, *8*, 4134–4139.

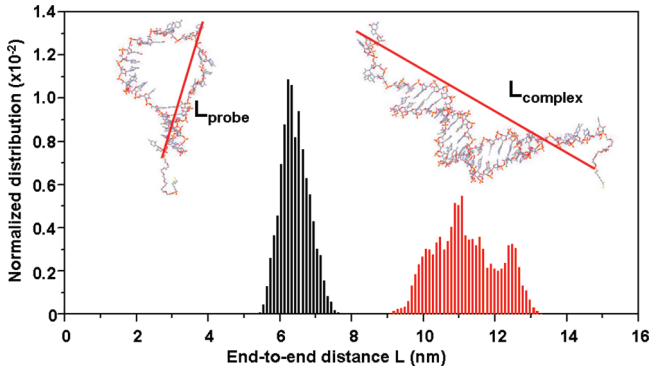

Figure 2. Normalized distributions of *L* during 3 ns MD simulations. *L* is defined as the maximum atom-to-atom distance from the phosphorus atom closest to the 5′-end. The black curve stands for the stem-and-loop structure of DNA-HP probe, and the red curve represents the open configuration in which a perfectly complementary sequence to the loop is H-bonded to give a double-stranded segment.

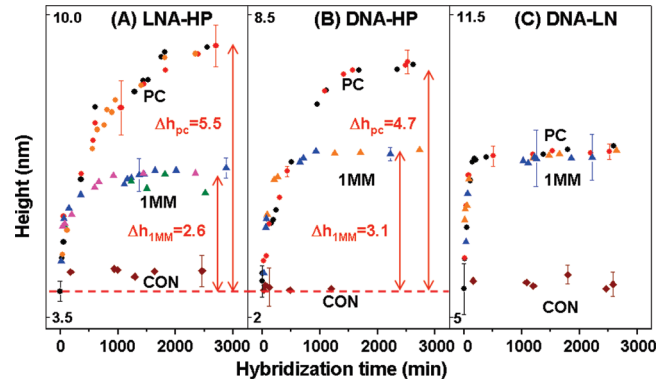

Figure 3. Kinetic profiles using AFM height to signal the extent of hybridization for recognition layers consisted of (A) LNA-integrated hairpin, (B) hairpin only, and (C) linear oligonucleotides. Symbols represent different target DNA molecules. The color-coded symbols indicate that each uptake curve may be constructed by experimental data collected from more than one gold substrate to ensure reproducibility. Errors correspond to the mean values and standard deviation of height obtained from at least three independent nanoshaved holes within the film.

the hybridization process (see Figure S1 in the Supporting Information). Here, we are interested in the depth profile generated from LNA-HP and DNA-HP using DNA-LN as the benchmark. Figure 1A displays the AFM topographic images of 0.8 μm × 0.8 μm flat areas covered by the above three probes under TE buffer. Nanoshaving was accomplished by sweeping a smaller area (300 nm × 300 nm) of the above films several times with the AFM tips under high vertical force. The grafted molecules were, thus, mechanically removed to expose the underlying gold substrate. Height-contrast measurements between the resulting square holes and the surrounding covered surfaces yield the different monolayer depths (the blue height profile in Figure 1C). The observed diversity in film thickness (LNA-HP 4.0 ± 0.2 nm, DNA-HP 2.4 ± 0.3 nm, DNA-LN 5.5 ± 0.5 nm) is likely due to variations in molecular shape (hairpin vs linear), orientation, and packing density. To be more specific, we can calculate the nominal, fully extended end-to-end distances of the linear and hairpin probes using 3.5 nm for the S-C_6-HEG spacer, 0.43 nm for each base in single-stranded DNA (ss-DNA) and 0.34 nm for each base pair in the double-stranded stem.[26] The molecular height of the 31-mer DNA-LN is, thus, about 16.8 nm. Regarding the hairpin structure, if we consider the length of the 19-mer single-stranded loop as its perimeter, the diameter of the loop is about 2.6 nm; therefore, the total height of the DNA-HP or LNA-HP is estimated to be 8.1 nm. Apparently, AFM rendered much reduced height values, presumably, a result of conformational folding and/or tip flattening. Nevertheless, the shorter dimensions of the hairpin-type films are not unexpected. The low experimental layer thickness can also be ascribed to the fact that the surface-tethered molecules are collectively oriented in a tilted manner, and relevantly, the packing density (surface coverage) can vary depending on how the strands align themselves toward the surface. Hybridization can be monitored in situ by injecting the required target solutions (4 μM in 137 mM NaCl-TE buffer[27]) into the AFM liquid cell and subsequently recording the thickness difference (Δh) resulting from the original or several freshly created nanoscale holes (images in Figure 1B were taken after ~40 h hybridization to ensure completeness), and the corresponding Δh's for each recognition layer challenged by the perfectly cDNA strand are demonstrated by the differences between the red and blue cursor plots in Figure 1C.

Notable thickness changes confirm that the interfacial layers experience considerable restructuring following the formation of more densely packed monolayers composed of an equilibrium mixture of hybridized and nonhybridized molecules. The larger Δh readouts for both LNA-HP and DNA-HP (unwinding of the stem-loop configuration), as compared to that for DNA-LN, establish that oligonucleotides with secondary structural features behave as more sensitive probes. The probe density effect can account for the smaller Δh (less complete target capture) of the linear ss-DNA probes because severe repulsive electrostatic and steric interactions impede hybridization at high coverages which can be as crowded as ~10^{13} molecules/cm^2.[28] In contrast, Keating and co-workers reported coverages of only ~10^{12} molecules/cm^2 for thiolated-DNA hairpin molecular beacon probes conjugated to metal nanowires.[15] In addition to the factor of probe density, Benight and co-workers observed a two times greater target accessibility to the hairpin compared to the linear probes, and they attributed this promotion to the increased stability of the hairpin probe/target duplex structure.[4] A generalized Born (GB) solvation model-based molecular dynamics (MD) simulations of DNA-HP and its hybridized DNA-HP/PC complex structures were performed in the NVT ensemble at 300 K with AMBER force field. The starting configurations were subjected to 3 ns of MD with a 1 fs time step, and 150 000 snapshots taken at 20 fs intervals were used to analyze the geometric size of the molecules. Assuming that the hybridization affects only the oligonucleotide part, regardless of variations of the S-C_6-HEG segment, normalized distributions of oligonucleotide end-to-end distance (L) for both the hairpin and the unraveled structures can be obtained, as shown in Figure 2. The mean values are 6.4 nm for the stem-and-loop

(26) Tinland, B.; Pluen, A.; Sturm, J.; Weill, G. *Macromolecules* **1997**, *30*, 5763–5765.

(27) The 137 mM salt concentration was chosen for giving the best signals; see: Castelino, K.; Kannan, B.; Majumdar, A. *Langmuir* **2005**, *21*, 1956.

(28) Peterson, A. W.; Heaton, R. J.; Georgiadis, R. M. *Nucleic Acids Res.* **2001**, *29*, 5163–5168.

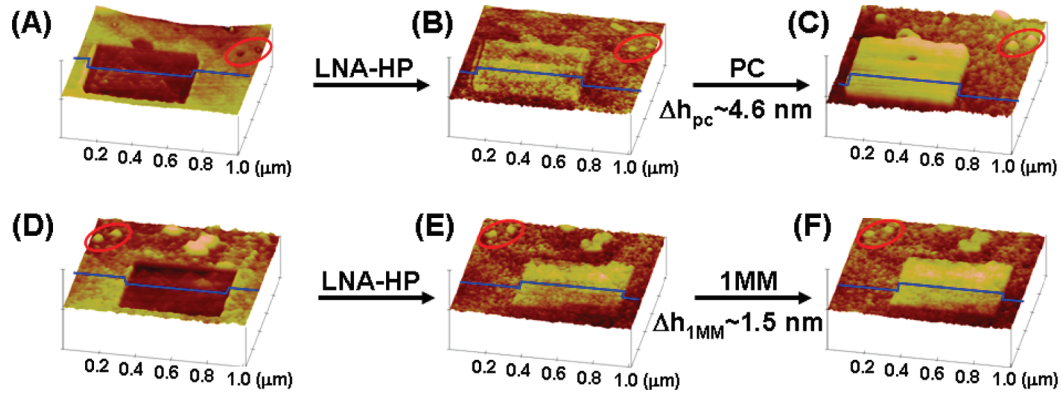

Figure 4. In situ AFM sequences of matrix nanoshaving, probe grafting, and target hybridization at side-by-side miniaturized LNA-HP spots challenged by PC (A)−(C) and 1MM (D)−(F), respectively.

framework $\langle L_{probe} \rangle$ and 11.2 nm for the open probe/target complex $\langle L_{complex} \rangle$. Thus, we acquire a theoretical height change $\Delta h = \langle L_{complex} \rangle - \langle L_{probe} \rangle = 4.8$ nm, in good agreement with the experimental findings (see Δh of DNA-HP in Figure 1C). Sferrazza and co-workers performed neutron reflection measurements on a monolayer of comparable thiolated hairpin DNA (a 6-mer double-stranded stem and a 16-mer loop) before and after hybridization with a cDNA target. They independently confirmed a substantial ~4 nm change of film thickness, indicative of the opening of stem-loop configuration toward helix formation upon molecular recognition.[29] It is noticeable that the even more elevated Δh (greater hybridization efficiency) gained in LNA-HP, against its DNA-HP counterpart, suggests that LNA-modification further enhances the function of apprehending the complementary targets. As Benight has proposed,[4] the stability difference between LNA-HP and DNA-HP (T_m = 61.4 °C vs 58.4 °C) may be the rationale for the improved binding event.

The ability to recognize single-base mismatches is the true paragon of DNA or RNA target detection. To test for single-base mismatch discrimination, the detailed course of hybridization was monitored by the time evolution of AFM imaging and height measurements of the nanoshaved indentations. Figure 3A shows the hybridization kinetic profiles of PC (solid circles), 1MM (solid triangles), and CON (solid diamonds) targets invading the LNA-HP probe layer under static conditions. The same procedure was applied to DNA-HP and DNA-LN, Figure 3B,C, under identical reaction conditions (targets, salt concentrations, and temperature) which allow for an unbiased comparison between responses to species with and without mismatches. The insignificant signal uptakes observed in the control experiments are to verify that Δh's are positively due to hybridization. In Figure 3C, a relatively rapid hybridization rate is observed and steady state is reached in less than 250 min. However, the equivalent maximal height achieved by both PC and 1MM represents that the linear probe is not selective enough to distinguish one A-C mismatch embedded in the sequence. In Figure 3B, signals from the DNA-HP probe show much slower approach to a plateau (>1000 min), which might be due to (1) the high activation barrier to the open configuration and/or (2) low surface concentration of the reacting DNA-HP molecules (perhaps in a lying-down configuration) reflected by the relatively small initial thickness of the self-assembled monolayer (only ~2.4 nm). Differentiable readouts between PC and 1MM, desirable for an intelligent probe, appear after 1000 min hybridization, reaching an ultimate discrimination ratio of 1.5/1 ($\Delta h_{PC}/\Delta h_{1MM}$) at an 2520 min interval. Even more interesting is the stark contrast observed in Figure 3A, where the LNA modification results in an appreciably reduced hybridization signals on exposure to 1MM targets, increasing the discrimination ratio $\Delta h_{PC}/\Delta h_{1MM}$ to at least 2.1/1 (the height still grows even after 2500 min in the case of PC) and outperforming the selectivity of DNA-HP. Such a sensor performance is comparable to the results achieved by fluorescence-based detection using surface immobilized molecular beacons which can distinguish a G-G mismatch out of a 24-base-pair target at room temperature.[30] The relatively high selectivity ($\Delta h_{PC}/\Delta h_{1MM}$) of LNA-HP can be rationalized to the interplay between maximizing the signal for Δh_{PC} as the substitution of LNA residues makes the hybridized duplex stiffer[31] and minimizing the signal for Δh_{1MM} as LNA imparts greater intolerance to the probe; therefore, a single mismatch suffices for significant destabilization of the heteroduplex. Furthermore, LNA-HP appears to identify the single-base mismatched targets more rapidly than its DNA-HP analog, evidenced by the earlier (500 min) signal saturation toward 1MM.

Hybridization of Individually Addressed Nanoscale Probe Spots. Assay miniaturization is advocated to improve surface-capture performance (cost and speed-to-answer). To this end, we fabricated nanofeatures (spot size: 500 nm × 500 nm) of tethered LNA-HP probe molecules within a biocompatible matrix of a prehybridized 12-mer thiolated double-stranded (ds) DNA (HS-C_6-HEG-5′-GATCCTCATCGA-3′/5′-TCGATGAGGATC-3′) on gold through sequential AFM nanoshaving and self-assembly. Direct comparison of hybridization with PC and 1MM targets can be made in situ on the same surface, and the discrimination ratio $\Delta h_{PC}/\Delta h_{1MM}$ can be determined from the AFM topographic change signals. Figure 4A shows a ~3.1 nm indentation created within the ds-DNA SAM by nanoshaving, representing the depth of the matrix and a height reference. After incubating the surface with LNA-HP (1 μM) for 60 min, the hole was filled and the height of the protrusion is approximately ~1.0 nm above the background

(29) Steichen, M.; Brouette, N.; Buess-Herman, C.; Fragneto, G.; Sferrazza, M. *Langmuir* **2009**, *25*, 4162–4167.

(30) Du, H.; Strohsahl, C. M.; Camera, J.; Miller, B. L.; Krauss, T. D. *J. Am. Chem. Soc.* **2005**, *127*, 7932–7940.

(31) LNA is an RNA mimic, and the persistence length of duplex RNA is 1.5−1.9 fold longer than that for DNA; see: Kebbekus, P.; Draper, D. E.; Hagerman, P. *Biochemistry* **1995**, *34*, 4354–4357.

in Figure 4B. After introduction of the PC target solution (4 μM) and 60 min hybridization, the height of the nanofeature increases to ~5.6 nm above the background 4(C). On its right, the same protocol was repeated to form an adjacent LNA-HP spot (using the red-circled mark as the reference position) which, instead, finishes up with an elevation of only ~2.5 nm after invasion of the 1MM target, Figure 4D−F. The clear difference between the two nanofeatures gives $\Delta h_{PC}/\Delta h_{1MM} \sim 3$ and reinforces that LNA-HP is indeed an arrayable and highly selective probe. When a surface density of $\sim 10^{12}$ molecules/cm^2 for the hairpin-type probes[15] and 100% hybridization efficiency is assumed, in such a 500×500 nm^2 spot area, there are only about several thousand captured target DNAs, capable of producing significant, discernible topographic changes.

CONCLUSION

In summary, deliberate stem-and-loop motif and strategically placed LNA modification at the triplet codon position are two indispensable components for a smart surface probe to elicit sufficient discriminatory power in SNP identification. The "change of thickness", a physical response inside the recognition monolayer or at the nanospot due to stem opening and duplex stiffening upon the interfacial probe−target hybridization, serves as a sensitive and selective readout that is readily detected by combining AFM nanolithography and imaging capabilities. The small number of molecules (as low as a few thousand) required to achieve the single-base mismatch recognition by this AFM-based methodology may open the way for screening nucleic acid targets in a miniaturized array format.

ACKNOWLEDGMENT

We thank the financial support from the National Science Council of the Republic of China under Contract No. 96-2628-M-110-006-MY2. C.-M.C. is grateful to Professor Gang-yu Liu at UC Davis for sharing her expertise in the AFM-based nanolithography.

SUPPORTING INFORMATION AVAILABLE

Calibration plots and exemplary in situ AFM image sequence in the course of surface hybridization. This material is available free of charge via the Internet at http://pubs.acs.org.

Received for review November 21, 2009. Accepted February 5, 2010.

AC902665C